

1 **Fast and easy disinfection of coronavirus-contaminated face masks using**  
2 **ozone gas produced by a dielectric barrier discharge plasma generator**

3  
4 Jinyeop Lee<sup>1+</sup>, Cheolwoo Bong<sup>1+</sup>, Pan K. Bae<sup>2</sup>, Abdurhaman T. Abafogi<sup>1</sup>, Seung H. Baek<sup>1</sup>, Yong-Beom  
5 Shin<sup>2,3,4</sup>, Moon S. Bak<sup>1,5,\*</sup>, and Sungsu Park<sup>1,5,6,\*</sup>

6  
7 <sup>1</sup>School of Mechanical Engineering, Sungkyunkwan University, Suwon 16419, Korea

8 <sup>2</sup>BioNano Health Guard Research Center (H-GUARD), Daejeon 34141, Korea

9 <sup>3</sup>Bionanotechnology Research Center, Korea Research Institute of Bioscience and Biotechnology  
10 (KRIBB),

11 Daejeon 34141, Korea

12 <sup>4</sup>Department of bioengineering, KRIBB School, University of science and Technology (UST), Daejeon  
13 34141,

14 Korea

15 <sup>5</sup>Biomedical Institute for Convergence at SKKU (BICS), Sungkyunkwan University, Suwon 16419,  
16 Korea

17 <sup>6</sup>Institute of Quantum Biophysics (iQB), Sungkyunkwan University, Suwon 16419, Korea

18  
19  
20 \* Each contributed equally to the work.

21 \*Correspondence and requests for materials should be addressed to M. S. Bak  
22 (moonsoo@skku.edu)/S. Park (nanopark@skku.edu).

23  
24  
25  
26  
27  
28  
29  
30  
31  
32  
33  
34  
35  
36  
37

38

39 **Abstract**

40 Face masks are one of the currently available options for preventing the transmission of the  
41 severe acute respiratory syndrome coronavirus 2 (SARS-CoV-2), which has caused the 2019  
42 pandemic. However, with the increasing demand for protection, face masks are becoming  
43 limited in stock, and the concerned individuals and healthcare workers from many countries  
44 are now facing the issue of the reuse of potentially contaminated masks. Although various  
45 technologies already exist for the sterilization of medical equipment, most of them are not  
46 applicable for eliminating virus from face masks. Thus, there is an urgent need to develop a  
47 fast and easy method of disinfecting contaminated face masks. In this study, using a human  
48 coronavirus (HCoV-229E) as a surrogate for SARS-CoV-2 contamination on face masks, we  
49 show that the virus loses its infectivity to a human cell line (MRC-5) when exposed for a  
50 short period of time (1 min) to ozone gas produced by a dielectric barrier discharge plasma  
51 generator. Scanning electron microscopy and particulate filtration efficiency (PFE) tests  
52 revealed that there was no structural or functional deterioration observed in the face masks  
53 even after they underwent excessive exposure to ozone (five 1-minute exposures).  
54 Interestingly, for face masks exposed to ozone gas for 5 min, the amplification of HCoV-229E  
55 RNA by reverse transcription polymerase chain reaction suggested a loss of infectivity under  
56 the effect of ozone, primarily owing to the damage caused to viral envelopes or envelope  
57 proteins. Ozone gas is a strong oxidizing agent with the ability to kill viruses on hard-to-  
58 reach surfaces, including the fabric structure of face masks. These results suggest that it may  
59 be possible to rapidly disinfect contaminated face masks using a plasma generator in a well-  
60 ventilated place.

61 Keyword: face mask, coronavirus, ozone gas, disinfection.

62

63

64

65

66

67

68

69

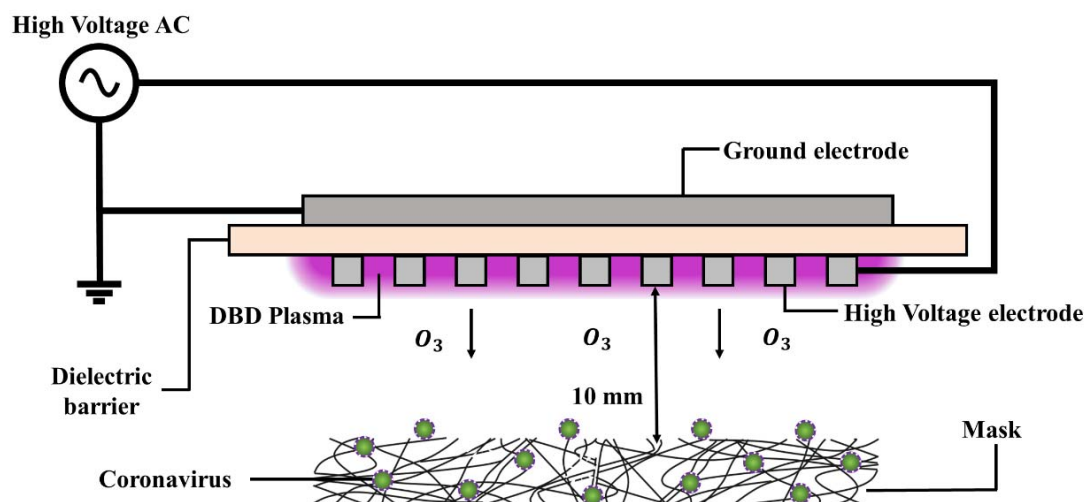
70

## 71 **Introduction**

72 Face masks are serving as one of the options for preventing severe acute respiratory  
73 syndrome coronavirus 2 (SARS-CoV-2), which has caused the 2019 international pandemic of  
74 the coronavirus disease.<sup>1</sup> However, with increasing demands for protection, face masks are  
75 becoming limited in stock; concerned individuals and healthcare workers from many  
76 countries are now facing the issue of the reuse of potentially contaminated masks in many  
77 countries. Thus, there is an urgent need to develop a fast and easy method of disinfecting  
78 contaminated face masks. There already exist technologies for the sterilization of medical  
79 equipment, including personal protective equipment (PPE); these technologies include  
80 autoclave treatment, ethylene oxide gassing, ionized hydrogen peroxide fogging and  
81 hydrogen peroxide vaporization.<sup>2</sup> However, most of them are not practical for disinfecting  
82 face masks with SARS-CoV-2.<sup>2</sup> It was reported that ozone gas produced by plasma generators  
83 can inactivate various types of viruses on different surfaces, including porous ones.<sup>3-6</sup> Ozone  
84 is a powerful oxidizing agent, but it does not linger. Its production, involving the use of  
85 electricity and a normal atmosphere, is easy and inexpensive. However, it has not been  
86 determined whether ozone gas can disinfect face masks contaminated with SARS-CoV-2  
87 without compromising the filtration efficiency of the masks.

88 Here we show that a human coronavirus (HCoV-229E)<sup>7,8</sup> as a surrogate for SARS-CoV-2  
89 on face masks lost its infectivity to a human cell line (MRC-5) when exposed to gaseous  
90 ozone produced by a dielectric barrier discharge (DBD) plasma generator<sup>9</sup> for a short time (1  
91 min) (Figure 1). Neither structural nor functional deterioration of the face masks even with  
92 excessive exposures (5 times, 5 min per each time) to the ozone were observed by scanning  
93 electron microscopy (SEM) and a particulate filtration efficiency (PFE) test. Interestingly, RNA  
94 of HCoV-229E on the face masks by the ozone for 5 min was amplified by reverse  
95 transcription polymerase chain reaction (RT-PCR). This is the first demonstration of the  
96 potential of using ozone gas for disinfecting face masks contaminated with a coronavirus.

97



98

99 Figure 1. A schematic diagram describing the disinfection of a face mask contaminated by a  
100 coronavirus using ozone produced by a DBD plasma generator. It consists of a high-voltage,  
101 high-frequency power supply and two electrodes separated by a 1 mm-thick alumina  
102 dielectric barrier. Plasma was produced on the face of the device with the perforated  
103 electrode, along the rims of the holes.

104

## 105 ■ RESULTS AND DISCUSSION

106 **Inhibitory effect of ozone gas on virus and bacteria on face masks.** Among the numerous  
107 types of plasma generators, the dielectric barrier discharge (DBD) plasma generator is  
108 considered the most energy-efficient and cost-effective plasma generator for ozone  
109 production; it forms ozone through the dissociation of molecular oxygen (O<sub>2</sub>) by collisions  
110 with excited electronic nitrogen populated by electron impacts and the ensuing combination  
111 between the atomic oxygen and O<sub>2</sub>.<sup>9</sup>

112 When face masks, experimentally contaminated with a human coronavirus (HCoV-  
113 229E)<sup>7,8</sup> as a surrogate, were exposed to ozone gas (about 120 ppm) produced by the  
114 plasma generator for either 1 or 5 min, no viable HCoV-229E was recovered from the face  
115 masks (Table 1). Corresponding untreated face masks showed the recovery of about 3 log  
116 units of tissue culture infective dose 50% (log TCID<sub>50</sub>) per mL following 15 min of air drying.  
117 To the best of our knowledge, this is the first demonstration of the potential of using ozone

118 gas for disinfecting face masks contaminated with a coronavirus. Similar results were  
119 obtained for face masks experimentally contaminated with either influenza A virus (H1N1)<sup>10</sup>  
120 (Table S1) or Gram-positive bacteria *Staphylococcus aureus* (Table S2 and Figure S1) when  
121 exposed to ozone gas. These results suggest that virus and bacteria on face masks can be  
122 inactivated by ozone gas at a concentration of about 120 ppm within a short time (1-5 min).

123

124 Table 1. HCoV-229E titer recovered from contaminated face masks with and without  
125 exposure to ozone gas.

Treatment of face masks <sup>a</sup> contaminated with HCoV-229E	Recovered virus <sup>b</sup> (log TCID <sub>50</sub> ± S.D.)
None	3.0 ± 0.2 (n = 4)
Ozone gas (120 ppm <sup>c</sup> , 1 min)	0 (n = 3)
Ozone gas (120 ppm, 5 min)	0 (n = 3)

126 <sup>a</sup>Samples (30 mm × 35 mm in size) were cut from face masks (Kleenguard®; product number  
127 Y2-44015, Kimberly-Clark Worldwide, Inc., Irving, TX, USA) with 3-layers filtering. The front  
128 side was sprayed with about 250 µL of HCoV-229E culture (about 4.5 log TCID<sub>50</sub> per mL) and  
129 dried at room temperature for 15 min in a biosafety cabinet before exposed to ozone gas.

130 <sup>b</sup>Virus particles on the samples were collected by washing the sample surface with 5 mL of  
131 PBS (phosphate buffered saline, pH 7.4) and measured using MRC-5 cells (ATCC, Bethesda,  
132 MD, USA).<sup>11</sup>

133 <sup>c</sup>The ozone concentrations produced by the DBD plasma generator were measured via UV  
134 absorption spectroscopy.<sup>12</sup>

135 n: sample number.

136

### 137 **Partial degradation of viral RNA by ozone gas**

138 To understand the mechanism underlying the viral inactivation of face masks by ozone gas,  
139 the experimentally contaminated face masks (Kleenguard®; product # Y2-44015, Kimberly-  
140 Clark Worldwide, Inc., Irving, TX, USA)—with and without exposure to ozone gas for 5 min—  
141 were washed, and the washing solutions were assayed with the quantitative reverse  
142 transcription polymerase chain reaction (qRT-PCR).<sup>13</sup> Surprisingly, there was no significant

143 difference ( $p > 0.05$ ; student's t-test) in the amount of amplifiable RNAs between the  
144 unexposed and exposed masks, indicating that the short exposure may not fully degrade the  
145 viral RNA (Table 2). Similarly, the RNA of either H1N1 (Table S3) or *S. aureus* (Table S4) on the  
146 face masks was not totally degraded by the exposure to ozone gas. These results suggest  
147 that the loss of infectivity could be due to the damage to the viral envelope or envelope  
148 proteins, resulting in failure of the virus to attach itself to host cells.<sup>14</sup>

149

150 Table 2: qRT-PCR of HCoV-229E in washing solutions obtained from contaminated face  
151 masks with and without exposure to ozone gas.

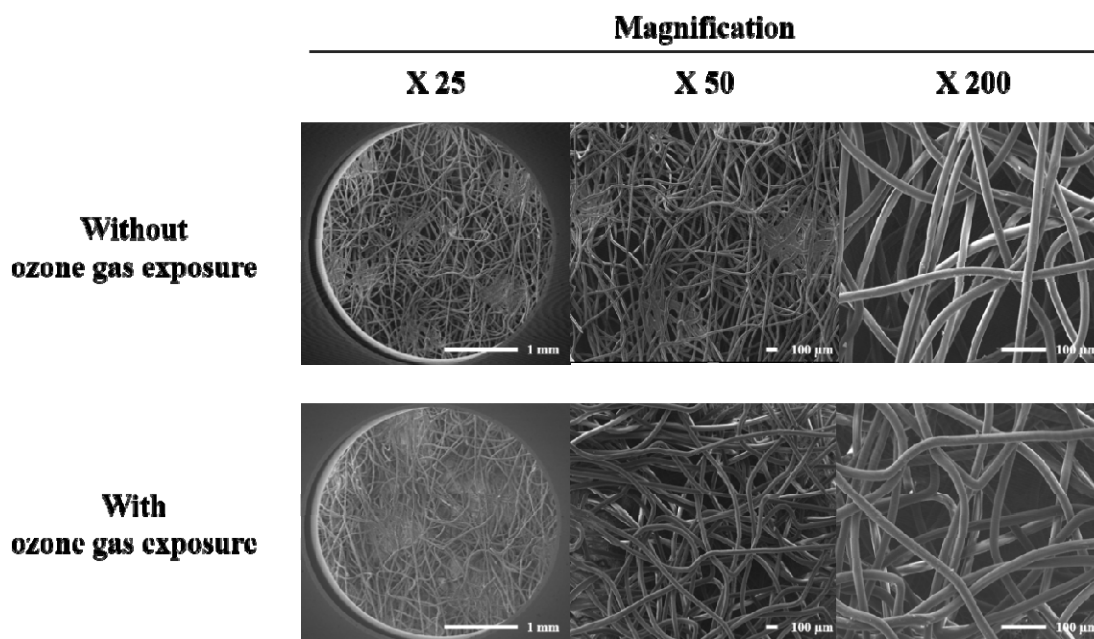
Treatment of face masks contaminated with HCoV-229E	Ct value <sup>a</sup> (mean $\pm$ S.D.)
None	22.7 $\pm$ 0.4 (n = 6)
Ozone gas (120 ppm, 5 min)	23.1 $\pm$ 0.6 (n = 6)

152 <sup>a</sup> cycle threshold (Ct) is defined as the number of cycles required for the fluorescent signal to  
153 exceed the background signal level (threshold). n: sample number.

154

#### 155 **No structural damage on the filter layer of face masks**

156 To test if the exposure of face masks (Kleenguard®) to either plasma or ozone gas causes  
157 any damage to their filter layer, uncontaminated face masks were exposed to ozone gas for  
158 5 min (five 1-minute exposures). We did not see any noticeable damage on the front and  
159 back side of the face masks with eyes and under a light microscope, either (data not shown).  
160 Their inner filter layer composed of polypropylene meltblown non-woven fabric was further  
161 examined under a SEM. As shown in Figure 2, there was no detectable structural damage  
162 caused to the filter layer of the exposed face masks. The result showed that the repeated  
163 exposures (5 times) of face masks to ozone gas did cause structural damage to the face  
164 masks.



165

166 Figure 2. Scanning electron microscopy images of the filter layer of uncontaminated face  
167 masks (Kleenguard®) with and without exposures to ozone gas for 5 min (five 1-minute  
168 exposures). The images were taken by a field-emission scanning electron microscope (FE-  
169 SEM-EDS, JSM7500F, JEOL Ltd., Tokyo, Japan).

170

#### 171 **No functional deterioration on face masks**

172 The electrocharged filter is an essential component of dust masks such as N95 and KF94  
173 masks and there was a concern that the charge on the filter could be lost with its exposure  
174 to ozone gas. The functioning of KF94 masks (registration number: F1-28712011; Kleannara  
175 Co., Seoul, Korea) which are certified to filter out 94% of particulate matter (about 0.4  $\mu\text{m}$   
176 diameter), after exposed to ozone gas for 5 min (five 1-minute exposures) was thus assessed  
177 using a standard test for measuring PFE with paraffin oil mists.<sup>15</sup> There was no statistical  
178 difference in PFE between the exposed and unexposed face masks (Table 3). Taken together  
179 with the SEM images, it is suggested that the repeated exposures (5 times) of face masks to  
180 ozone gas do not cause structural or functional damage to the face masks.

181

182

183

184 Table 3: PFE of uncontaminated face masks (KF94) with and without exposure to ozone gas.

Certified testing lab <sup>a</sup>	Ozone gas treatment on uncontaminated face masks	PFE (%) <sup>b</sup> (Mean ± S.D.)
FITI Testing & Research Institute	None	98.5 ± 1.3 (n=3)
	Ozone gas (120 ppm, 5 min)	99.3 ± 1 (n=3)
Korea Mask Laboratory	None	98.4 ± 0.5 (n=6)
	Ozone gas (120 ppm, 5 min)	98.6 ± 0.5 (n=6)

185 <sup>a</sup> The lab is certified and registered as a testing lab by the ministry of food and drug safety  
186 (MFDS) in Korea.

187 <sup>b</sup> Measured by a standard method using paraffin mist. n: sample number.

188

## 189 ■ CONCLUSIONS

190 In this study, using a human coronavirus (HCoV-229E) as a surrogate for SARS-CoV-2  
191 contamination on face masks, the virus is shown to lose its infectivity to a human cell line  
192 (MRC-5) when exposed for a short period of time (1 min) to ozone gas produced by the DBD  
193 plasma generator. SEM and PFE tests revealed that there was no structural or functional  
194 deterioration observed in the face masks even after they underwent excessive exposure to  
195 ozone (five 1-minute exposures).

196 Ozone gas is a strong oxidizing agent with the ability to kill viruses on hard-to-reach  
197 surfaces, including the fabric structure of face masks. Inexpensive consumer-grade ozone  
198 generators are widely available. Our results suggest that it may be possible to rapidly  
199 disinfect face masks contaminated with SARS-CoV-2 using a plasma generator in a well-  
200 ventilated place.

201

## 202 ■ MATERIALS AND METHODS

### 203 DBD plasma generator

204 The plasma generator consists of a high-voltage, high-frequency generator (Minipuls 2.2;  
205 GBS Elektronik GmbH, Großberkmannsdorf, Germany) and two electrodes separated by a 1  
206 mm -thick alumina dielectric barrier. Each electrode was made of a perforated stainless-steel  
207 plate and bare aluminum tape. The plasma was produced only at the perforated electrode,  
208 along the rims of the holes. As the dielectric barrier allows electrons and ions to accumulate  
209 on the surface, preventing the transition from a cold plasma to an arc, a sinusoidal voltage  
210 was applied to steadily produce the plasma (Figure S2). The plasma was turned on for 1 min



211 after every 4 min to avoid any damage resulting from thermal heating.

### 212 **UV absorption spectroscopy**

213 The ozone concentrations produced by the DBD plasma generator were measured via UV  
214 absorption spectroscopy.<sup>16</sup> Light from a mercury lamp (BHK 90-0005-01, spectral line: 253.65  
215 nm) was collimated using lenses and an optical fiber and sent through a gas medium, 4.3 cm  
216 above the electrode surface where the plasma is produced. The transmitted light intensity  
217 was then measured using a spectrometer (AvaSpec-2048L). As the wavelength-dependent  
218 absorption cross section of ozone is broad near 253.65 nm and known as  $1.137 \cdot 10^{-17}$   
219  $\text{cm}^2\text{molecule}^{-1}$ , the ozone concentration can be evaluated by the Beer-Lambert law  
220 described as follows:

$$n_{O_3} = -\frac{1}{\sigma_{O_3}L} \ln\left(\frac{I}{I_0}\right) \quad (1)$$

221 where  $I$  and  $I_0$  are the transmitted and incident light intensities;  $n_{O_3}$  is the number density of  
222 ozone;  $\sigma_{O_3}$  is the ozone absorption cross-section near 253.65 nm;  $L$  is the optical path  
223 length. The ozone concentrations under the test conditions were determined to be  
224 approximately 120 ppm.

### 225 **Coronavirus culture**

226 HCoV-229E was cultured using human fetal lung fibroblast cell (MRC-5; ATCC, Bethesda, MD,  
227 USA) in a 96-well plate.<sup>11</sup>

### 228 **Exposure of face masks experimentally contaminated with HCoV-229E to ozone gas**

229 Samples ( $n = 6$ ) were cut (30 mm  $\times$  35 mm in size) from face masks and sprayed with about  
230 250  $\mu\text{L}$  of HCoV-229E culture (4.5 log TCID<sub>50</sub> per mL) in a biosafety cabinet at a biosafety  
231 level-2 (BSL-2) laboratory while wearing face masks and gloves. The samples were then  
232 dried for 15 min at 25 °C and were individually exposed to ozone for both 1 and 5 min using  
233 the plasma generator (Figure 1) in a chemical hood.

### 234 **Determination of TCID<sub>50</sub> value**

235 Immediately after the exposure, the virus particles on the samples were collected by  
236 washing the samples with 5 mL of PBS (phosphate buffered saline, pH 7.4). TCID<sub>50</sub> was  
237 determined by adding serial 10-fold dilutions of HCoV-229E collected from each mask into a

238 human fetal lung fibroblast cell (MRC-5, ATCC, Bethesda, MD, USA) monolayer in a 96-well  
239 plate.<sup>11</sup> The plates were observed for cytopathic effects for 4 days. The viral titer was  
240 calculated via the Reed and Munch endpoint method.<sup>11</sup> Viral titer collected from the face  
241 masks was measured using MRC-5 cells (ATCC, Bethesda, MD, USA).<sup>11</sup>

#### 242 **RT-PCR**

243 Immediately after the exposure, the virus particles on the samples were collected by  
244 washing the samples with 5 mL of PBS. qRT-PCR was performed using StepOne™ Real-Time  
245 PCR system (Applied biosystems, CA, USA) and MG 2X One Step RT-PCR SYBR® Green Master  
246 Mix reagents (Cancer Rop Co Ltd., Seoul, Korea). A segment of the *N* gene of HCoV229E was  
247 amplified using a forward primer (CGCAAGAATTCAGAACCAGAG) and a reverse primer  
248 (GGCAGTCAGTTCTTCAACAA)<sup>13</sup> with an amplicon size of 83 bp (Bioneer, Daejeon, Korea).  
249 The thermocycler conditions were as follows: reverse transcriptase at 50 °C for 30 min and  
250 an initial denaturation at 95 °C for 5 min, followed by 45 cycles of denaturation at 95 °C for  
251 15 s, annealing at 52 °C for 30 s, and an extension at 72 °C for 30 s. To confirm that the target  
252 amplicon was properly formed, a melting curve analysis was conducted. The fluorescence  
253 intensity was measured within the range of 60–95 °C at a rate of 0.2 °C/s.

#### 254 **SEM**

255 A field-emission scanning electron microscope (FE-SEM-EDS, JSM7500F, JEOL Ltd., Tokyo,  
256 Japan) was used to take images of untreated and treated masks (n=4). To obtain the  
257 morphology of the electrostatic melt blown filter layer, which is the middle layer of the face  
258 mask, the melt blown filter was cut to obtain a 5 mm x 5 mm sample that was coated with  
259 iridium (Ir) for 15 minutes via the ion sputtering method. The FE-SEM-EDS was operated at  
260 15 kV, and the working distance (WD) was 8 mm. All the sample images were acquired with  
261 magnification factors of 25, 50, and 200.

#### 262 **Paraffin Oil Test**

263 The standard test for measuring the filtration efficiency with paraffin oil mist was performed  
264 on masks at FITI Testing & Research Institute (Cheongju, Korea) and Korea Mask Laboratory  
265 (KML; Hanam city, Korea), the authorized testing organizations in Korea. In this test, a tester  
266 first produces paraffin oil mist with a particle size ranging from 0.05 to 1.7 µm, 0.4 µm on  
267 average.<sup>15</sup> The flow containing the paraffin oil aerosol at a concentration of  $20 \pm 5 \text{ mg/m}^3$  is

268 then blown towards the mask at a flow rate of 95 L/min. The filtration efficiency, given by Eq.  
269 (2), is then evaluated by measuring the concentrations of paraffin oil mist upstream and  
270 downstream of the mask. The efficiency is a value averaged over 30 s and must be measured  
271 within 3 min after the test starts.

$$P = \frac{C_1 - C_2}{C_1} \times 100 \quad (2)$$

272 where  $P$  is the filtration efficiency;  $C_1$  and  $C_2$  are the concentrations of paraffin oil mist  
273 upstream and downstream of the mask, respectively.

274

275 **Supplementary Materials:** Supplementary materials can be found at  
276 [www.mdpi.com/xxx/s1](http://www.mdpi.com/xxx/s1).

277 **Acknowledgements:** We thank Ms. J. So for giving an idea for the project.

278 **Funding:** S.P. was supported by the BioNano Health-Guard Research Centre as a Global  
279 Frontier Project (H-guard 2018M3A6B2057299) through the National Research Foundation  
280 (NRF) of Ministry of Science and ICT (MSIT) in Korea. M.S.B. was supported by a grant  
281 through a future integration program of Kangbuk Samsung Hospital-Biomedical Institute for  
282 Convergence (BICS) at Sungkyunkwan University.

283 **Conflicts of Interest:** The authors declare no conflict of interest.

284

285

286

287

288

289

290

291

292

293

294

295

296

297

298 **References**

299 1. Leung NHL, Chu DKW, Shiu EYC, et al. Respiratory virus shedding in exhaled breath  
300 and efficacy of face masks. *Nat Med*. 2020. doi:10.1038/s41591-020-0843-2.

301 2. Kumar A, Kasloff SB, Leung A, et al. N95 Mask Decontamination using Standard  
302 Hospital Sterilization Technologies. Preprint. Posted online April 08, 2020. MedRxiv.  
303 doi:10.1101/2020.04.05.20049346.

304 3. Hudson JB, Sharma M, Vimalanathan S. Development of a practical method for using  
305 ozone gas as a virus decontaminating agent. *Ozone Sci Eng*. 2009;31(3):216-223.  
306 doi:10.1080/01919510902747969.

307 4. Zimmermann JL, Dumler K, Shimizu T, et al. Effects of cold atmospheric plasmas on  
308 adenoviruses in solution. *J Phys D Appl Phys*. 2011;44(50):505201. doi:10.1088/0022-  
309 3727/44/50/505201.

310 5. Mastanaiah N, Johnson JA, Roy S. Effect of dielectric and liquid on plasma sterilization  
311 using dielectric barrier discharge plasma. *PLoS One*. 2013;8(8):e70840  
312 doi:10.1371/journal.pone.0070840.

313 6. Morfill GE, Shimizu T, Steffes B, Schmidt HU. Nosocomial infections—a new approach  
314 towards preventive medicine using plasmas. *New J Phys*. 2009;11(11):115019..

315 7. Van Der Hoek L, Pyrc K, Berkhout B. Human coronavirus NL63, a new respiratory  
316 virus. *FEMS Microbiol Rev*. 2006;30(5):760-773. doi:10.1111/j.1574-  
317 6976.2006.00032.x.

318 8. Wentworth D, Holmes KV. Molecular determinants of species specificity in the  
319 coronavirus receptor aminopeptidase N (CD13): influence of N-linked glycosylation. *J*  
320 *Viro*. 2001;75(20):9741-9752. doi:10.1128/JVI.75.20.9741-9752.2001.

321 9. Stefanovic I, Bibinov N, Deryugin A, et al. Kinetics of ozone and nitric oxides in  
322 dielectric barrier discharges in O<sub>2</sub>/NO<sub>x</sub> and N<sub>2</sub>/O<sub>2</sub>/NO<sub>x</sub> mixtures. *Plasma Sources Sci*  
323 *Technol*. 2001;10(3):406.

324 10. Dotis J, Roilides EJH. H1N1 Influenza A infection. *Hippokratia*. 2009;13(3):135-138.

- 325 11. Reed LJ, Muench H. A simple method of estimating fifty per cent endpoints. *Am J*  
326 *Epidemiol.* 1938;27(3):493-497. doi:10.1093/oxfordjournals.aje.a118408.
- 327 12. Reuter S, Winter J, Iseni S, et al. Detection of ozone in a MHz argon plasma bullet jet.  
328 *Plasma Sources Sci Technol.* 2012;21(3):034015.
- 329 13. Lu R, Yu X, Wang W, et al. Characterization of human coronavirus etiology in Chinese  
330 adults with acute upper respiratory tract infection by real-time RT-PCR assays. *PLoS*  
331 *One.* 2012;7(6):e38638 doi:10.1371/journal.pone.0038638.
- 332 14. Tseng C, Li C. Inactivation of surface viruses by gaseous ozone. *J Environ Health.*  
333 2008;70(10):56-63.
- 334 15. Choi HW, Yoon S, Lee JH, et al. Comparison of pressure drop and filtration efficiency  
335 of particulate respirators using welding fumes and sodium chloride. *Ann. Occup. Hyg.*  
336 2011;55(6):666-680. doi: 10.1093/annhyg/mer032.
- 337 16. Orphal J, Staehelin J, Tamminen J, et al. Absorption cross-sections of ozone in the  
338 ultraviolet and visible spectral regions: Status report 2015. *J Mol Spectrosc.*  
339 2016;327:105-121. doi: 10.1016/j.jms.2016.07.007.
- 340